Biogeochemistry (2020) 148:169–189
https://doi.org/10.1007/s10533-020-00652-z

Aggregate formation and organo-mineral association affect characteristics of soil organic matter across soil horizons and parent materials in temperate broadleaf forest

S. Vormstein · M. Kaiser · H.-P. Piepho · B. Ludwig

Received: 26 August 2018 / Accepted: 3 March 2020 / Published online: 13 March 2020

Abstract Precise assessment of soil organic carbon (OC) storage requires understanding of soil type and depth specific differences in organic matter (OM) stabilization. Therefore, we aimed to analyze OC dynamics down the soil profile and to clarify the effect of depth on the importance of aggregate formation and mineral adsorption for OC storage in mature beech forest soils developed from different parent materials. Aggregate size and density fractions were separated from samples of top and subsoil horizons, which were quantified and analyzed by infrared spectroscopy. We also determined the microbial biomass C (C_{mic}) and the amount of C decomposed within incubation experiments (CO_2-C) for the bulk soil samples. OC stabilized via aggregate formation and mineral association significantly increased with soil depth. However, this stabilized pool seemed to fuel the labile OM stronger in the subsoil than in the topsoil because the CO_2-C/SOC and CO_2-C/C_{mic} ratios increased with depth. Measured differences in the magnitude of the detected stabilization and destabilization patterns were attributed to parent material and soil horizon, indicating pronounced spatial and vertical heterogeneity in the contribution of soils under temperate broadleaf forest to terrestrial C sequestration. Considering such site and depth specific differences will improve assessment and modelling of soil OC storage for areas covered with the same forest type but with high pedogenetic diversity.

Keywords Soil organic matter stabilization · Forest soil · Soil parent material · Soil genetic horizons · Aggregate size fraction · Density fraction

Responsible Editor: Susan E. Crow.

S. Vormstein · B. Ludwig
Department of Environmental Chemistry, University of Kassel, Nordbahnhofstr. 1a, 37213 Witzenhausen, Germany

M. Kaiser (✉)
Department of Agronomy and Horticulture, University of Nebraska - Lincoln, 202 Keim Hall, Lincoln, NE 68583, USA
e-mail: mkaiser6@unl.edu

H.-P. Piepho
Institute of Crop Science, University of Hohenheim, Biostatistics Unit, Fruwirthstr. 23, 70599 Stuttgart, Germany

Introduction

Forest topsoils and subsoils account for approximately 70% of the global soil organic C (SOC) leading to their large importance for terrestrial ecosystem services such as the mitigation of climate change (Vancampenhout et al. 2012). Topsoils (i.e., A horizons) usually show distinctly higher SOC concentrations than subsoils but 30 to 63% of the total SOC is stored at a soil depth of 30–100 cm. Even in depths between 100 and 200 cm up to 40% of the total SOC can be found

(Batjes 1996; Angst et al. 2016). However, Mobley et al. (2015) pointed out that 90% of 360 studies, analyzed in two review articles about the impact of land use on SOC (Post and Kwon 2000; West and Post 2002), only sampled to a depth of 30 cm or less. For two other reviews on the impact of land use on organic carbon (OC) in tropical soil (Don et al. 2011; Powers et al. 2011), the average sampling depth was 39 and 14.6 cm across 158 and 80 studies, respectively (Wade et al. 2019). Consequently, uncertainties about subsoil OC cycling are generally larger as compared with the topsoil and subsoil OC dynamics cannot be deduced from that in the topsoil because the environmental conditions differ widely (e.g. Rasse et al. 2006; Rumpel and Kögel-Knabner 2011).

For soils under forest, bioclimatic characteristics such as boreal coniferous or temperate broadleaf (Post et al. 1982) and soil mineral characteristics, determined by the parent material the soil has developed from (Kaiser et al. 2012), were identified as major driving factors for OC storage and cycling. However, quantitative understanding of organic matter (OM) decomposition and stabilization in topsoils and subsoils that have developed from different parent materials under specific bioclimatic forest types is in critical need to assess OC storage capacities and predict changes more precisely (Rumpel and Kögel-Knabner 2011; Vancampenhout et al. 2012; Gabriel et al. 2018). For the long-term (> 100 years) stabilization of OM against microbial decomposition, which is especially important for mitigating climate change, the association of OM with mineral compounds and the occlusion in aggregates were shown to be crucial (Schmidt et al. 2011; Kleber et al. 2015). The capability of soils to protect OM against biological decomposition by the formation of aggregates and organo-mineral associations depends on mineral characteristics, such as the content of reactive Fe- and Al-oxides, polyvalent cations, and layer silicates (Baldock and Skjemstad 2000; Eusterhues et al. 2005; Mikutta et al. 2006). These mineral characteristics are in turn affected by the parent material the soil has developed from and by pedogenetic processes responsible for the formation of different soil horizons along the soil profile. Consequently, it can be expected that the rates and mechanisms of OM stabilization depend on the soil parent material as well as on specific characteristics of pedogenetic soil horizons (Kaiser et al. 2011, 2012).

In general, it can be assumed that with increasing soil depth the organic compounds are getting smaller and more reactive towards charged mineral surface sites because of the ongoing oxidative breakdown (microbial processing) (Kramer et al. 2012; Kleber et al. 2015). Consequently, it is postulated that with increasing soil depth smaller aggregates (< 53 µm) and organo-mineral associations become increasingly important for the OM stabilization at the cost of larger aggregates (> 53 µm) (Paul et al. 2001; Kaiser et al. 2002; Rasse et al. 2006). Because organo-mineral associations and aggregates < 53 µm have been shown to protect OM more efficiently than aggregates > 53 µm (e.g., Feng et al. 2016), a stronger OM stabilization can be expected in the subsoil compared to the topsoil. However, it is critical to quantify this for soils developed from different parent materials because the specific horizons that have evolved differ regarding their vertical transport rates of dissolved OM and their support of root growth, which can affect in turn the patterns of soil aggregation and organo-mineral associations (Torres-Salan et al. 2018).

To analyse the contributions of larger aggregates, smaller aggregates, and organo-mineral associations for OM storage and stabilization along the soil profile, different fractionation schemes can be applied. Density fractionation of soil offers a procedure to assess the interaction between OM and the mineral phase by separating the bulk soil OM into the free light fraction (flF: not aggregate occluded organic particles, i.e. plant residues), the aggregate occluded light fraction (olF: aggregate occluded organic particles or plant residues), and the mineral-associated OM (heavy fraction: HF) (Cerli et al. 2012; Schrumpf et al. 2013). The OM associated with the olF and HF is generally more degraded, smaller in size, and more stabilized than the OM associated with the flF (Wagai et al. 2009; Schrumpf and Kaiser 2015). Complementary to density fractionation, the separation of water-stable aggregate size fractions by a wet-sieving procedure from soil reveals information about the relevance of aggregate formation at different scales for the OM storage and stabilization in different soil depths (e.g., John et al. 2005).

Recent studies on OM stabilization in soils under temperate broadleaf forest using aggregate (Sánchez-de León et al. 2014) or density fractionation (McFarlane et al. 2013) schemes focused solely on topsoil, which does not allow for conclusions on OM subsoil

dynamics. Studies that expanded to the subsoil usually fractionated samples from fixed depth increments to analyze differences between forest topsoil and subsoil (Schrumpf et al. 2013; Angst et al. 2016). This might lead to the mixing of material from different horizons that differ in OM and mineral characteristics, impeding the elucidation of horizon specific OM stabilization patterns. For temperate broadleaf forest, studies quantifying the relative importance of OM stabilization mechanisms in pedogenetic horizons of soils developed from different parent material are missing to the best of our knowledge. Such horizon and soil parent material specific data would help to improve the prediction and modelling of fluctuations in atmospheric CO_2 concentrations resulting from changes in forest SOC due to changes in climate and land use (e.g., Jain and Yang 2005; Gabriel et al. 2018).

Objectives of this study were (i) to determine how well bulk SOC content and mineral characteristics describe the OC contents associated with aggregate size and density fractions and with microbial biomass in topsoil versus subsoil horizons, (ii.1) to clarify whether the relative OC proportions associated with aggregate size classes and density fractions differ significantly between different pedogenetic horizons of soils under temperate broadleaf forest differing in parent material, and (ii.2) how this affects depth specific OM decomposition dynamics. To achieve this, we sampled material from pedogenetic horizons, down to the parent material, of five soils in central Germany that have developed from different parent materials in similar climate and that are covered with mature beech forest. From these soil samples, we separated three density and four aggregate size fractions indicative for different degrees and mechanisms of OM stabilization against microbial decay. These fractions were also characterized by Fourier transform infrared (FTIR) spectroscopic analyses providing information about the amount of C=O groups shown to be crucial in the formation of organo-mineral associations and aggregates and being affected by microbial processing and microbially derived OM (Kaiser et al. 2012, 2014). We also determined for all bulk soil samples the microbial biomass C (C_{mic}) and the amount of organic C respired as CO_2 within 7 and 14 days to quantify soil horizon specific differences in microbial activity and the amount of the most labile OM.

We hypothesize (i) that mineral characteristics and bulk SOC content are useful to quantitatively describe contents of OC in aggregate size and density fractions but that mineral characteristics are better predictors for the subsoil, (ii.1) a significant decrease of OC associated with macro-aggregates (> 250 µm) and free, organic particles with depth and a significant increase of OC associated with minerals, and (ii.2) that this increase in more protected OM with depth will lead to lower total and relative amounts of easily decomposable OC.

Materials and methods

Study sites and soil sampling

We analyzed five soils in central Germany near the city of Göttingen (Germany) that have developed from different parent material namely Shell Lime Stone (coordinates: 51° 32′ 43.69″ N, 10° 02′ 34.95″ E), Basalt (coordinates: 51° 28′ 35.60″ N, 09° 45′ 32.46″ E), Red Sandstone (coordinates: 51° 34′ 45.89″ N, 10° 03′ 59.52″ E), Tertiary Sand (coordinates: 51° 26′ 25.64″ N, 09° 41′ 24.25″ E), and Loess (coordinates: 51° 34′ 51.52″ N, 10° 14′ 43.03″ E). The study sites were located at a distance between 10 km (Lime Stone) and 27 km (Loess) from Göttingen with an elevation between 200 m (Loess) and 470 m (Basalt) above sea level. All sites were covered with mature beech forest showing a stand age between 95 years (Loess) and 166 years (Lime Stone). The sites were part of the research project SUBSOM, which was a collaborative effort of ten universities and research institutes from across Germany aimed at elucidating the OM storage and turnover in subsoil (www.subsom.de). Parameters such as stand age and parent material were determined within a general characterization of the study sites. First characteristics of the study sites have been published by Angst et al. (2018). The climatic data for the study sites were generated from www.worldclim.org (Hijmans et al. 2005). The mean annual precipitation and mean annual surface temperature for the site with the Loess soil were 733 mm and 8.5 °C, for the Tertiary Sand soil 799 mm and 8.4 °C, for the Lime Stone soil 906 mm and 8.4 °C, for the Basalt soil 968 mm and 7.7 °C, and for the Red Sandstone soil 794 mm and 8.3 °C.

To cover a wide range in soil mineral characteristics shown to be relevant for OM stabilization, we sampled soils developed on distinctly different parent

materials. It has to be noted that replicate profiles at different sites with the same parent materials could not be included. Details about parent material, soil classification, pedogenetic horizons and their depth distribution can be found in Table 1. In May 2014, three soil pits of each site were excavated and samples were taken by horizons down to the parent material. For each horizon and each pit, we took soil material from each of the four walls and combined them into one sample. Thus we had three field replications per horizon and site.

Physico-chemical soil characterization

A subsample of each field moist sample was sieved < 2 mm to conduct the following analyses. The soil texture was determined by wet sieving and the pipette method according to DIN ISO 1277 (2002). The pH values were measured in 0.01 M $CaCl_2$ (25 ml $CaCl_2$: 10 g soil) with a glass electrode (pH electrode BlueLine 14 pH, Schott Instruments, Mainz, Germany). For the determination of exchangeable Na^+, K^+, Ca^{2+}, Mg^{2+} and Al^{3+}, the soil (oven dry, 40 °C) was slowly leached with 0.1 M barium chloride (soil:solution ratio 1:10). Cations were measured in the filtered extracts by the use of ion chromatography (850 Professional IC, 237 Metrohm, Herisau, Switzerland). The cation exchange capacity (CEC) was calculated by the sum of the exchangeable cations and the data were normalized to 105 °C dry soil.

Contents of oxalate-soluble iron and aluminum were determined in slight modification according to DIN 19684-6 (1997). Briefly, 2.5 g field moist soil were extracted in 50 ml extraction solution (one part 0.1 M ammonium oxalate solution and 0.765 parts 0.1 M oxalic acid) by horizontal shaking for two hours and afterwards filtered. The filtrates were measured with an atomic absorption spectrometer (906 AA, GBC, Melbourne, Australia) and the results were calculated based on soil dry mass. The measurements of dithionite-soluble iron and aluminum were done according to Mehra and Jackson (1960). Briefly, 2 g field moist soil were treated with a mixture composed of 40 ml 0.3 M Na-citrate solution and 10 ml 1 M sodium bicarbonate solution, heated to 70 °C before 1 g Na-dithionite was added. After the reaction time of

Table 1 Parent material (Soil), soil classification, soil horizon classification (Horizon) and horizon specific depth ranges for soil sampling for the five investigated sites

Soil	Soil classification[a]	Horizon[a]	Depth ranges for soil sampling (cm)	
			Upper	Lower
Shell Lime Stone	Eutric Cambisol	Ah	0	10
		BwAh	10	30–50
Basalt	Eutric Cambisol	Ah	0	10
		BwAh	10	40–60
		Bw	40–50	80
Red Sandstone	Dystric Cambisol	Ah	0	5–8
		BwAh/Bw*	5–8	43–50
		Bw	43–50	70–90
Tertiary Sand	Dystric Brunic Arenosol	AhE	0	7–10
		BwAh	7–10	20–30
		Bw	20–30	63–70
		2C	63–70	140–150
Loess	Haplic Luvisol/Eutric Cambisol*	Ah	0	5–10
		E/BwE*	5–10	45–50
		Bt/E2/Bwt*	45–50	75–85
		C	80–85	170–180

*The differences in the classification of soil type and soil horizons within same sites result from the heterogeneity in the field

[a]Classification according to IUSS 2006

2 h with regular stirring, the samples were left to cool and then centrifuged at 3000×*g* (Multifuge 3 S-R, Heraeus, Hanau, Germany). This procedure was repeated up to three times until the soil was grey. The remaining soil was treated with 40 ml 0.1 M magnesium sulfate, stirred, centrifuged and added to the extraction solution. This solution was filled up with deionized water to 250 ml. Dithionite-soluble iron and aluminum were also measured using AAS (see above) and the data were normalized to 105 °C dry soil.

The bulk soil, the aggregate size fractions, and the heavy fraction were ball-milled, whereas the light fractions (see below for further details) and fractions with low yields were ground in an agate mortar by hand. Total C and N concentrations of all samples were analyzed by dry combustion (Elementar, Vario El, Hanau, Germany) where the total C content corresponds to the bulk SOC content and OC content of the fractions because no carbonates were detectable using a "Scheibler" apparatus (Loeppert and Suarez 1996). For the separated aggregate size and density fractions (explained below), the OC contents (g OC kg^{-1} fraction) and the dry mass yield of each fraction (g fraction kg^{-1} soil) were used to calculate the OC content for each fraction in g OC kg^{-1} soil. The contents of C_{mic} were determined by the chloroform-fumigation-extraction method (Brookes et al. 1985; Vance et al. 1987; Wu et al. 1990).

Soil respiration was determined as described by Heinze et al. (2011). Briefly, 60 g of field moist soil were adjusted to 50% of the water holding capacity and incubated together with 5 ml of 0.5 M NaOH in a separate vessel, which was replaced after 7 days, in 1 l glass jars for two weeks at 22 °C (Kühlbrutschrank ICP 750, Memmert, Schwabach, Germany). Each horizon specific sample from each soil pit was incubated in three laboratory replicates, which were used to calculate mean values for the respective field replicate. After the addition of 3 ml of 0.5 M $BaCl_2$ and three drops of phenolphthalein to the NaOH-solution the evolved CO_2 was determined by titration with 0.5 M HCl to pH 8.3 (Isermeyer 1952).

Separation of aggregate size and density fractions

Water stable aggregates of all soil samples were fractionated using a wet-sieving method developed by Cambardella and Elliot (1993) and slightly modified by Jacobs et al. (2009). Briefly, 40 g of air-dried soil (< 10 mm) were placed on a 1000 µm sieve and soaked in deionized water for 10 min to allow slaking. Floating organic particles were skimmed off separately and discarded. Afterwards the sieve was lifted out of the water until the water had run off. The sieve was re-submerged and lifted out again for 50 repetitions. The soil/water suspension passing the sieve was transferred onto the next smaller sieve and the fractionation procedure was continued as described above. The used mesh sizes were: 1000 µm for large water-stable macro-aggregates, 250 µm for small water-stable macro-aggregates and 53 µm for water-stable micro-aggregates. For each fraction, the soil/water suspension passing the 53 µm sieve (silt, clay and very small micro-aggregates) was recollected, vacuum-filtered (< 0.45 µm), dried at 40 °C and weighed. Due to operator variability (Jacobs et al. 2010), the whole fractionating procedure was carried out by a single person after 25–30 test runs to ensure individual reproducibility.

Density fractionation (Golchin et al. 1994; Jacobs et al. 2009) was applied to all soil samples. We conducted a series of pre-tests to define the most suitable experimental setting with respect to the density cut offs used to separate the flF and the olF and the amount of ultrasonic energy applied to disperse aggregates before the olF was separated (Cerli et al. 2012). The tested densities of the sodium polytungstate solution (SPT) ranged between 1.6 and 2.0 g cm^{-3} for both the flF and the olF and the tested ultrasonic energies ranged between 200 and 800 J cm^{-3}. The power output of the ultrasonic device (Digital Sonifier 250, Converter model 102C, Branson Utrasonics, Danburry, USA) and sonication settings were determined according to North (1976). For all samples, the most suitable density cut off was 1.8 g cm^{-3} to separate the flF and the olF.

Ultrasonic energies applied to the soil/water suspensions varied between 200 J cm^{-3} for the Tertiary Sand, 400 J cm^{-3} for the Loess and the Red Sandstone, 600 J cm^{-3} for the Basalt, and 800 J cm^{-3} for the Shell Lime Stone. Briefly, 6 g field moist soil sieved < 2 mm were placed in a 70 ml centrifugation tube and 30 ml of SPT were added. The tube was then gently shaken manually five times upside down. The suspension was then allowed to settle down for 30 min before it was centrifuged for 30 min at 4000×*g*. The supernatant with the floating particles was decanted and vacuum filtered (< 0.45 µm) and, afterwards,

washed with 2 l deionized water to obtain the flF. The remaining soil pellet was transferred into a 50 ml glass beaker, mixed with 30 ml SPT and subsequently sonicated with the energies given above to disperse the aggregates and release the occluded particulate OM. During sonication, the samples were cooled (< 45 °C) with crushed ice surrounding the beaker. After disaggregation, the suspension was transferred back in the 70 ml centrifugation tube, allowed to settle down for 30 min, and centrifuged at $4000 \times g$. The supernatant was decanted and the soil pellet was again mixed with 30 ml SPT, centrifuged and decanted, this process was then repeated one more time. The decanted supernatants were combined, filtered and washed as described above to obtain the olF. The remaining soil pellet represents the HF. To clean the HF from the remaining SPT as completely as possible, the pellet was suspended in 1.5 l deionized water. To precipitate the HF, 0.5 M $AlCl_3$ solution (2.5 ml to 1 l suspension) was added. The water was siphoned off and the HF was also vacuum filtered (< 0.45 µm: the filters were changed in case of pore clogging, which was only in few cases necessary) and washed with 0.5 L deionized water. All fractions were dried at 40 °C and weighed.

FTIR spectroscopic analyses

The composition of the OM associated with the aggregate size fractions and the HF was evaluated using diffuse reflectance infrared spectroscopy (DRIFT) (Tensor 27, BRUKER, Ettlingen, Germany). The FTIR spectrum of each sample, which was ground using a ball mill, was recorded in the range of wave numbers from 850 to 4000 cm^{-1} at resolution of 4 cm^{-1} by performing 200 scans using the Easy Diff unit (Pike Technologies, Madison, USA). Using the subroutine from OPUS 7.5 software (Bruker, Ettlingen Germany), all spectra were smoothed once and then baseline corrected. The heights of the absorption maxima (wavenumbers 2904–2908 cm^{-1} and 2876–2836 cm^{-1}) in the "aliphatic" region, representing hydrophobic C-H groups were added (band "A") and related to the maximum signal height at 1645–1605 cm^{-1} (band "B") representing hydrophilic C=O functional groups in soil OM (Ellerbrock and Gerke 2013; Kaiser et al. 2014). Several parameters are related to the height of the absorption maxima of band "B": (i) the abundance of ionizable carboxyl groups and the resulting CEC of the OM in the sample, (ii) the hydrophilicity and the polarity of the OM in the sample, and (iii) the abundance of proteinaceous material such as microbial debris. By relating the "C=O" region to the "aliphatic" region of the FTIR spectrum, we thus obtain a numerical parameter "B/A" that allows a semi-quantitative comparison of samples.

Statistical analyses

A mixed effects model was fitted to each site to study the effect of soil depth on the relative contributions of aggregate size and the density fractions to SOC and on the B/A ratios using the mixed model (MIXED) procedure of the SAS University edition (SAS Institute Inc. 2014). The models included a fixed effect of depth. The residual error was modelled to have a compound symmetry structure for observations down the same soil pit (Piepho et al. 2004) (implemented using the REPEATED statement and specifying soil pit as subject effect). In four cases (B/A ratios: aggregate size fractions 1000–250 µm, 250–53 µm, and < 53 µm and HF of the Basalt site), an autoregressive model (AR(1)) had to be assumed to achieve convergence. The estimation procedure was restricted maximum likelihood and the denominator degrees of freedom were estimated using the Kenward-Roger method. Studentized residuals were inspected for homoscedasticity and normality. In six cases (OC in % of SOC of the aggregate size fraction < 53 µm of the Red Sandstone site, B/A ratio of the aggregate size fraction < 53 µm of the Basalt site, B/A ratio of the aggregate size fraction < 53 µm of the Tertiary Sand site, and B/A ratios: aggregate size fractions 1000–250 µm and 250–53 µm and HF of the Loess site), a log transformation of the response variable was performed to achieve normality and homoscedasticity. In cases of a significant depth effect, a Tukey test was carried out to compare depth means.

Regression analyses were carried out to study how well SOC content and mineral characteristics describe the OC contents associated with aggregate size and density fractions and with microbial biomass. Analyses were conducted with the statistical software R (Version 3.4.0; R Development Core Team 2017). Multiple linear regression analyses with stepwise variable selection were carried out using mixed effects models for the response variables SOC, C_{mic} and the

OC contents in different fractions. For each depth, the entire data set consisting of all sites was used in the regression analyses. Regressions were carried out using the lme() command of the nlme package. Site was included as random effect. The Akaike information criterion was used to simplify models. Predictors were only considered in the final models in case of significant ($p \leq 0.05$) contributions. Residuals were inspected for normality (graphically and using the Shapiro–Wilk test) and homoscedasticity (graphically). The regression analyses were carried out separately for the topsoil soil horizon (five sites, n = 3 per site) and first subsoil horizon (five sites, n = 3 per site) of the five soils. The second and the third subsoil horizon were not considered, because the second subsoil horizon was only present in four soils and the third subsoil horizon were only present in two soils, which lowers the predictive power and comparability to the analyses including data from all soils.

For SOC, initial predictors were contents of Fe_{ox}, Al_{ox}, clay, and silt (Baldock and Skjemstad 2000; Eusterhues et al. 2005; Mikutta et al. 2006) in the subsoil horizon and model simplification resulted in Fe_{ox} as final significant predictor. This predictor was also significant for the topsoil horizon.

The initial model for C_{mic} in the subsoil horizon consisted of the predictors SOC and clay, since both may affect C_{mic} (Ren et al. 2019). The final model, after model simplification, had SOC as a significant predictor. The optimal model for the topsoil horizon had log-transformed (ln) C_{mic} as response variable and also SOC as significant predictor.

The contents of SOC, silt, clay, Fe_{ox}, and Al_{ox} were tested as predictors for the OC contents associated with the aggregate size and density fractions, since these variables are related to SOC stabilization (Baldock and Skjemstad 2000; Eusterhues et al. 2005; Mikutta et al. 2006). Model simplifications resulted only for olF in final models with significant predictors. These were SOC and Fe_{ox} in the subsoil and topsoil horizon.

The mixed effects models, with the fixed effects and random intercept, were compared with the respective null models, which included only the random intercept by computing analysis of variance tables for the fitted model objects using the anova() command in R. The mixed effects models, with fixed effects and random intercept, were significantly better than the respective null models.

Results

Physico-chemical soil characteristics

The clay contents covered a total range from 3.8% to 39.9% and increased among parent materials in the sequence Tertiary Sand < Red Sandstone < Loess ≤ Basalt < Lime Stone for the topsoil horizon and the first subsoil horizon, which were the only horizons present in all soils. The silt contents were lowest for the Tertiary Sand soil but, in contrast to the clay contents, highest for the Basalt and the Loess soil (Table 2). The generally acidic pH values (< 5) followed no clear pattern and varied between 3.2 for the topsoil horizon (0–7/10 cm) of the Tertiary Sand soil and 4.9 for the second subsoil horizon (40/50–80 cm) of the Basalt soil (Table 2).

The oxalate and dithionite soluble soil Fe contents (Fe_{ox} and Fe_{dith}) indicative for poorly and stronger crystalline Fe-oxides followed a different pattern compared to the clay and silt contents and generally increased in the sequence Tertiary Sand < Red Sandstone < Loess < Lime Stone < Basalt soil for the topsoil horizon and the first subsoil horizon. The data varied in total between 0.1 and 8.3 g kg^{-1} for Fe_{ox} and between 2.9 and 24.5 g kg^{-1} for Fe_{dith} (Table 2). The differences for the Al_{ox} (0.3 and 3.3 g kg^{-1}) and Al_{dith} (0.7 and 5.0 g kg^{-1}) contents were smaller than those found for the respective Fe contents. Across soil horizons, we found the lowest Al_{ox} and Al_{dith} contents in the Loess, Tertiary Sand or Red Sandstone soil and the highest in the Basalt or Lime Stone soil (Table 2).

Similar to the texture data and the oxalate as well as dithionite soluble Fe and Al contents, the CEC followed no clear pattern related to the soil depth/horizon. Especially the depth distribution for the Loess soil is here noteworthy because of the distinct higher CEC in the deepest subsoil horizon (69.4 mmol kg^{-1} in 80/85–170/180 cm) compared to the topsoil horizon (52.7 mmol kg^{-1} in 0–5/10 cm). The CEC varied in the topsoil between 44.4 mmol kg^{-1} (Tertiary Sand) and 139.8 mmol kg^{-1} (Lime Stone) and in the subsoil between 8.2 mmol kg^{-1} (second subsoil horizon, 20/30–63/70 cm, Tertiary Sand) and 122.5 mmol kg^{-1} (first subsoil horizon, 10–30/50 cm, Lime Stone) (Table 2).

Independent of the soil parent material, the SOC content of the pedogenetic horizons decreased with increasing soil depth. For the topsoil horizon, the SOC

Table 2 Parent material (Soil) and the sampling depth (Depth), texture (Sand, Silt, Clay), pH, contents of oxalate- and dithionite-soluble iron (Fe_{ox}, Fe_{dith}) and aluminium (Al_{ox}, Al_{dith}), cation exchange capacity (CEC), contents of bulk soil organic carbon (SOC) and nitrogen (N), OC/N-ratios (CN), contents of microbial biomass C (C_{mic}) as well as cumulative amounts of respired CO_2 after 7 and 14 days of the samples from the analyzed soil horizons of the five study sites

Soil	Depth	Sand		Silt		Clay		pH		Fe_{ox}		Fe_{dith}		Al_{ox}		Al_{dith}	
	[cm]	[%]								[g kg^{-1}]							
Shell Lime Stone	0–10	2.2	(0.40)	65.2	(3.61)	32.6	(3.23)	4.5	(0.14)	2.6	(0.59)	13.8	(1.97)	2.5	(0.32)	4.1	(0.44)
	10–30/50	1.1	(0.39)	58.9	(4.23)	39.9	(4.00)	4.4	(0.18)	1.9	(0.29)	15.0	(1.33)	3.3	(0.72)	4.7	(0.63)
Basalt	0–10	4.3	(0.04)	77.2	(2.29)	18.5	(2.33)	3.5	(0.13)	8.3	(1.37)	24.1	(1.02)	3.3	(0.45)	5.0	(0.59)
	10–40/60	6.1	(1.00)	72.4	(3.11)	21.5	(3.02)	4.2	(0.19)	7.0	(1.33)	24.5	(0.29)	3.0	(0.68)	4.5	(0.70)
	40/50–80	4.6	(0.06)	79.6	(3.66)	15.8	(3.60)	4.9	(0.16)	3.5	(0.15)	22.6	(6.53)	0.9	(0.10)	1.9	(0.18)
Red Sandstone	0–5/8	67.5	(0.48)	22.4	(0.87)	10.2	(0.82)	4.3	(0.21)	1.3	(0.05)	5.3	(0.10)	0.6	(0.02)	1.0	(0.07)
	5/8–43/50	67.3	(0.49)	23.6	(1.11)	9.0	(0.67)	4.1	(0.12)	1.4	(0.11)	5.4	(0.23)	1.2	(0.28)	1.4	(0.14)
	43/50–70/90	78.5	(4.87)	11.5	(1.06)	10.0	(3.82)	3.9	(0.01)	0.7	(0.41)	8.4	(0.78)	0.7	(0.16)	1.1	(0.14)
Tertiary Sand	0–7/10	78.2	(0.21)	16.1	(1.41)	5.7	(1.21)	3.2	(0.00)	1.1	(0.13)	4.6	(0.08)	0.7	(0.01)	1.3	(0.06)
	7/10–20/30	80.5	(0.81)	13.3	(0.29)	6.2	(0.59)	3.7	(0.11)	2.0	(0.10)	5.1	(0.17)	1.4	(0.12)	1.9	(0.20)
	20/30–63/70	84.4	(0.88)	10.9	(1.62)	4.7	(0.84)	4.2	(0.01)	1.1	(0.12)	3.9	(0.15)	1.7	(0.12)	1.9	(0.09)
	63/70–140/150	92.6	(0.70)	3.6	(1.11)	3.8	(1.35)	4.0	(0.01)	0.1	(0.04)	2.9	(0.16)	0.3	(0.05)	0.7	(0.08)
Loess	0–5/10	9.2	(2.63)	75.0	(4.19)	15.8	(1.95)	4.1	(0.15)	2.2	(0.17)	6.8	(0.33)	1.1	(0.09)	1.8	(0.21)
	5/10–45/50	8.8	(2.06)	76.0	(2.40)	15.2	(1.15)	3.7	(0.03)	2.1	(0.15)	7.2	(0.55)	1.2	(0.11)	2.1	(0.10)
	45/50–75/85	5.7	(1.87)	73.7	(2.32)	20.6	(3.26)	3.9	(0.05)	2.2	(0.33)	8.2	(0.51)	1.2	(0.04)	2.3	(0.11)
	80/85–170/180	15.2	(4.73)	67.5	(4.44)	17.3	(0.29)	4.2	(0.08)	1.0	(0.09)	8.8	(0.84)	0.8	(0.14)	1.9	(0.11)

Soil	CEC		SOC		N		CN—ratio		C_{mic}		Basal respiration			
											After 7 days		After 14 days	
	[mmol kg^{-1}]		[g kg^{-1}]						[mg kg^{-1}]		[g CO_2-C kg^{-1}]			
Shell Lime Stone	139.8	(16.2)	52.8	(4.75)	3.5	(0.26)	15	(0.47)	1149.1	(138.5)	96.6	(3.65)	177.8	(10.0)
	122.5	(37.4)	14.1	(1.90)	1.1	(0.19)	13	(0.56)	186.8	(72.3)	25.7	(4.43)	46.5	(6.3)
Basalt	104.4	(17.2)	104.3	(13.73)	6.6	(0.94)	16	(0.35)	2685.7	(968.4)	160.5	(15.41)	302.5	(32.3)
	52.6	(5.0)	23.2	(4.62)	1.8	(0.44)	13	(0.74)	233.0	(32.0)	22.3	(2.80)	41.2	(5.8)
	89.5	(26.2)	3.5	(0.02)	0.3	(0.00)	12	(0.09)	35.5	(6.2)	9.4	(0.07)	18.4	(0.4)
Red Sandstone	60.4	(6.5)	35.5	(3.59)	2.2	(0.20)	16	(0.21)	606.0	(86.1)	89.4	(5.26)	172.2	(4.9)
	24.2	(5.4)	6.5	(0.44)	0.4	(0.03)	16	(0.20)	129.0	(44.5)	11.0	(1.50)	18.2	(3.5)
	26.9	(7.9)	1.1	(0.14)	0.2	(0.03)	6	(0.06)	115.5	(82.8)	6.1	(0.70)	7.8	(1.8)

Table 2 continued

Soil	CEC		SOC	N		CN—ratio	C_{mic}		Basal respiration			
									After 7 days		After 14 days	
	[mmol kg^{-1}]		[g kg^{-1}]				[mg kg^{-1}]		[g CO_2-C kg^{-1}]			
Tertiary Sand	44.4	(3.5)	70.0	(5.81)	3.6	(0.27)	20	(0.24)	1254.1	(132.5)	156.4	(32.56)	287.1	(55.0)
	28.2	(4.3)	17.7	(1.85)	0.8	(0.10)	21	(0.28)	130.8	(22.4)	18.2	(2.93)	30.7	(5.0)
	8.2	(0.6)	3.6	(0.80)	0.3	(0.05)	13	(0.67)	26.9	(7.2)	4.5	(0.71)	10.4	(3.8)
	8.9	(1.1)	0.4	(0.01)	0.0	(0.00)	9	(0.43)	12.0	(1.4)	2.0	(0.43)	8.5	(1.5)
Loess	52.7	(9.3)	23.4	(1.61)	1.6	(0.13)	14	(0.27)	521.8	(58.9)	55.8	(5.70)	109.2	(11.7)
	35.0	(4.1)	7.7	(0.18)	0.5	(0.02)	15	(0.66)	108.8	(14.9)	8.7	(3.77)	13.5	(3.9)
	50.5	(15.9)	3.2	(0.10)	0.2	(0.02)	13	(1.15)	24.6	(4.9)	5.1	(0.54)	8.0	(0.5)
	69.4	(4.4)	2.3	(0.90)	0.2	(0.01)	9	(2.76)	11.9	(3.3)	8.7	(0.97)	11.8	(1.5)

The presented data are mean values of the replicated field samples and the standard erros are given in paranthesis (n = 3, except Basalt 40/50–80 and Loess 80/85–170/180: n = 2)

covered a range from 23.4 to 104.3 g kg^{-1} and increased in the sequence Loess < Red Sandstone < Lime Stone < Tertiary Sand < Basalt. A similar sequence was detected for the first subsoil horizon showing a total range from 6.5 to 23.2 g kg^{-1} with the difference that the Red Sandstone soil had here the lowest and the Loess soil had the second lowest SOC content. Remarkable appears the high SOC content in the first three horizons in the Tertiary Sand soil in comparison to the other soils, which cannot be explained by the differences in soil mineral characteristics (Table 2). The N contents for the topsoil horizon ranged from 1.6 to 6.6 g kg^{-1} and followed the same sequence as found for SOC. For the first subsoil horizons, the N contents varied between 0.4 (Red Sandstone) and 1.8 g kg^{-1} (Basalt) and were $\leq$ 0.3 g kg^{-1} in the further subsoil horizons (Table 2).

The C_{mic} contents as well as the basal respiration after 7 days and after 14 days generally decreased with increasing soil depth (Table 2). Similar to the respective topsoil OC and N data, the C_{mic} contents and the basal respiration after 7 and 14 days increased in the sequence Loess < Red Sandstone < Lime Stone < Tertiary Sand < Basalt. However, this sequence in parent materials could not be found for the CO_2-C and C_{mic} data detected for soil samples from the first subsoil horizon (Table 2).

In contrast to the CO_2-C emissions and the C_{mic} contents, the CO_2-C/SOC (mg CO_2-C kg^{-1} soil/mg OC kg^{-1} bulk soil) and CO_2-C/C_{mic} (mg CO_2-C kg^{-1} bulk soil/mg C_{mic} kg^{-1} soil) ratios generally showed for the subsoil horizons of all study sites the reverse trend resulting in distinct differences between the topsoil horizon (depth range 0–10 cm) and the deepest subsoil horizon of the Loess and the Tertiary Sand soil (depth range 70–180 cm). For the topsoil horizon (n = 5), the means and standard errors of the CO_2-C/SOC and CO_2-C/C_{mic} ratios were 0.0041 (± 0.0004) and 0.21 (± 0.03). The mean values and standard errors for the first (n = 5), second (n = 4), and third (n = 2) subsoil horizon for the CO_2/SOC ratios were, respectively, 0.0023 (± 0.0003), 0.0047 (± 0.0013), and 0.0134 (± 0.0071) and these for the CO_2/C_{mic} ratios were 0.23 (± 0.05), 0.37 (± 0.08), and 0.85 (± 0.13).

Aggregate size and density fractions

We separated four aggregate size fractions (> 1000 µm, 1000–250 µm, 250–53 µm, < 53 µm) from the topsoil and subsoil horizons of the five soils by wet-sieving. The OC contents (unit for all OM fractions if not otherwise stated: g OC kg^{-1} soil) of the two macro-aggregate fractions (> 1000 µm and 1000–250 µm) separated from the topsoil horizon ranged from 9.1 (Loess) to 45.7 g kg^{-1} (Basalt). The respective values for the micro-aggregate fractions (250–53 µm and < 53 µm) were distinctly lower and ranged from 0.22 (Red Sandstone) to 15.4 g kg^{-1} (Basalt) (Table 3). For the first subsoil horizon, which was also present in all five soils, the OC contents of the macro-aggregate fractions varied between 0.19 g kg^{-1} (Loess) and 14.3 g kg^{-1} (Tertiary Sand) and those of the micro-aggregate fractions between 0.22 g kg^{-1} (Tertiary Sand) and 6.5 g kg^{-1} (Basalt) (Table 3). The OC content of all of the remaining fractions of the second and third subsoil horizons ranged from 0.00 to 2.3 g kg^{-1}.

The density fractionation resulted in the flF, the olF and the HF for each of the soil horizons of the five soils. For the topsoil horizon, the OC content of the flF ranged from 0.78 (Loess) to 36.7 g kg^{-1} (Basalt) and from 6.5 (Loess) to 28.8 g kg^{-1} (Tertiary Sand) for the olF. The HF varied between 5.7 g kg^{-1} (Tertiary Sand) and 35.2 g kg^{-1} (Basalt). The respective differences in the subsoil horizons were much smaller for the flF and olF (0.00 to 4.1 g kg^{-1}) but remained relative high for the HF (0.28 to 18.6 g kg^{-1}) (Table 3). We detected in general the highest OC contents for the HF compared to flF and olF in the analyzed soil horizons with exception of the topsoil horizon of the Basalt and Tertiary Sand soil. Here we found OC contents of 36.7 g kg^{-1} (Basalt) and 33.3 g kg^{-1} (Tertiary Sand) for the flF and OC contents of 26.4 g kg^{-1} (Basalt) and 28.8 g kg^{-1} (Tertiary Sand) for the olF (Table 3). For the topsoil of the Tertiary Sand, it was remarkable that the flF and the olF contained about six times more OC than the HF (5.7 g kg^{-1}). Similar to the aggregate size fraction, we detected a general decrease in the OC contents of the density fractions with increasing depth (Table 3).

FTIR spectroscopic analyses

The aggregate size fractions and the HF from density fractionation were analyzed using FTIR spectroscopy resulting in information about the functional composition of the OM expressed as the B/A ratio. The B/A ratio allowed for a semi quantitative comparison of the amount of reactive C=O groups of the OM associated with aggregate size and density fractions separated from the topsoil and subsoil horizons of the five soils under study. The B/A ratios revealed for the aggregate size fractions generally increased with decreasing soil depth independent from the soil parent material and the size of the fraction (Fig. 1).

The HF showed a similar pattern as the aggregate size fractions with a general increase of the B/A ratio with increasing depth at least to the third subsoil horizon independent from the soil parent material (Fig. 1). Similar to the aggregate size fractions, the differences in the B/A ratio found for the HF (8.2 (Basalt) to 52.8 (Tertiary Sand)) of the topsoil horizon were smaller than those detected for the subsoil horizons (22.3 (10–50 cm, Basalt) and 162.6 (80–170 cm, Loess)).

Mixed effects models

For the topsoil and subsoil horizons, we aimed to describe SOC contents using mixed effects models with site as random intercept. The models for the topsoil and subsoil had Fe_{ox} as fixed effect and described the variability of SOC well (the Pearson correlation coefficient r between measured and modelled SOC was 0.97 for the topsoil and 0.98 for the subsoil) and the root mean squared errors (RMSE) were 6.9 and 1.5 g kg^{-1}, respectively. The modelling performance of the mixed effects models for log-transformed C_{mic} was markedly better in the topsoil (SOC, r = 0.95, RMSE = 0.2) than in the subsoil (SOC, r = 0.63, RMSE = 58.4). Agreements between modelled and measured organic C separated with the olF were good in the topsoil (r = 0.94, RMSE = 3.2 g kg^{-1}) and subsoil (r = 0.98, RMSE = 0.2 g kg^{-1}, Table 4, Fig. 2).

A mixed effects model was used for each site to analyze the effect of soil depth (i) on the relative proportions of SOC associated with the separated aggregate size and density fractions and (ii) on the B/A ratios revealed from the DRIFT spectra of the

Table 3 Contents of organic carbon (OC) associated with aggregate size fractions and density fractions in different sampling depths of the five sites given as mean values of the replicated field samples from the analyzed soil horizons of the five study sites

Soil		Aggregate size fractions								Density fractions					
	Depth	> 1000 µm		1000–250 µm		250–53 µm		< 53 µm		flF		olF		HF	
	[cm]	[g OC kg^{-1}]								[g OC kg^{-1}]					
Shell Lime Stone	0–10	34.67	(7.74)	10.80	(1.81)	1.92	(0.50)	0.58	(0.19)	1.85	(0.27)	18.27	(2.28)	27.93	(3.80)
	10–30/50	9.04	(3.26)	2.84	(1.09)	0.81	(0.26)	0.25	(0.08)	0.92	(0.10)	3.84	(0.30)	9.63	(1.59)
Basalt	0–10	24.41	(10.15)	45.65	(8.52)	15.44	(5.05)	1.86	(0.07)	36.70	(13.80)	26.38	(1.81)	35.20	(2.50)
	10–40/60	3.16	(1.07)	11.73	(1.23)	6.53	(2.19)	1.04	(0.33)	1.19	(0.38)	2.82	(0.39)	18.61	(4.32)
	40/50–80	0.39	(0.18)	1.22	(0.05)	1.43	(0.15)	0.51	(0.02)	0.27	(0.21)	0.19	(0.06)	3.07	(0.08)
Red Sandstone	0–5/8	24.17	(5.83)	10.44	(2.71)	2.71	(1.45)	0.22	(0.02)	5.30	(1.64)	12.39	(3.91)	14.92	(0.66)
	5/8–43/50	1.57	(0.37)	1.59	(0.20)	1.61	(0.11)	0.35	(0.04)	1.19	(0.13)	2.19	(0.12)	3.59	(0.10)
	43/50–70/90	0.24	(0.07)	0.13	(0.03)	0.41	(0.06)	0.20	(0.06)	0.14	(0.08)	0.09	(0.02)	0.78	(0.11)
Tertiary Sand	0–7/10	23.08	(4.50)	34.71	(8.70)	5.23	(0.81)	0.46	(0.13)	33.29	(2.27)	28.82	(6.28)	5.65	(0.60)
	7/10–20/30	1.65	(0.26)	14.32	(2.63)	2.28	(0.17)	0.22	(0.02)	4.10	(0.40)	3.85	(0.60)	9.42	(0.65)
	20/30–63/70	0.12	(0.04)	2.30	(0.47)	1.08	(0.30)	0.06	(0.01)	0.68	(0.40)	1.36	(0.50)	2.48	(0.57)
	63/70–140/150	0.02	(0.02)	0.10	(0.01)	0.23	(0.01)	0.05	(0.03)	0.00	(0.00)	0.00	(0.00)	0.28	(0.07)
Loess	0–5/10	9.07	(0.38)	9.28	(2.02)	1.99	(0.46)	0.80	(0.04)	0.78	(0.27)	6.49	(1.03)	14.07	(0.82)
	5/10–45/50	0.19	(0.03)	4.03	(0.28)	1.41	(0.13)	0.48	(0.03)	0.95	(0.02)	1.61	(0.07)	3.54	(1.09)
	45/50–75/85	0.03	(0.02)	0.48	(0.12)	1.12	(0.15)	0.33	(0.07)	0.57	(0.06)	0.92	(0.51)	2.09	(0.35)
	80/85–170/180	0.00	(0.00)	0.10	(0.03)	0.64	(0.06)	0.31	(0.03)	0.00	(0.00)	0.46	(0.07)	0.95	(0.01)

Standard errors given in parentheses (n = 3, except Basalt 40/50–80 and Loess 80/85–170/180 n = 2). The data are mean values of the replicated field samples and the standrad erros are given in paranthesis

aggregate size fractions and the HF. The results in Figs. 1 and 3 showed soil parent material specific significant changes in these parameters with soil depth, which is discussed in the following.

Fig. 1 Ratio of the maxima of absorption band B (hydrophilic ▶ C=O groups) and A (hydrophobic C–H groups) (i.e. B/A ratio) revealed from the infrared spectra of the aggregate size fractions and the density fractions that were separated from the horizon specific soil samples of the five study sites. Error bars are standard errors from three field replicates (except Basalt 40/50–80 and Loess 80/85–170/180 with n = 2). Different letters indicate significant differences between depths

Discussion

Bulk SOC

Site and poorly crystalline Fe-oxides exerted a strong positive effect on SOC storage in top and subsoil under mature beech forests, which is in agreement with findings from previous studies (e.g., Wiseman and Püttmann 2006; Zhao et al. 2016). Models that included site and poorly crystalline Fe-oxides were significantly better than those, which included only site. However, one has to keep in mind that significance of a predictor in a study with observational data is never a proof of causality. The detected strong effect of poorly crystalline Fe-oxides on the bulk SOC can be

Table 4 Linear regressions for different response variables by additionally considering the sites. The equations are the results of stepwise model simplifications. Only regression terms with significant contributions were considered. Units for the regression terms are kg g^{-1} multiplied by the unit given in the first column

Response variable	Random intercept	Regression terms
	Topsoil	
SOC [g OC kg^{-1}]	Basalt: 36.52 g kg^{-1}	+ 8.09 * Fe_{ox}
	Loess: 7.51 g kg^{-1}	
	Red Sandstone: 25.22 g kg^{-1}	
	Shell Lime Stone: 31.69 g kg^{-1}	
	Tertiary Sand: 59.00 g kg^{-1}	
Ln(C_{mic}) [ln(mg kg^{-1})]	Basalt: 5.81	+ 0.02 * SOC
	Loess: 5.81	
	Red Sandstone: 5.81	
	Shell Lime Stone: 5.81	
	Tertiary Sand: 5.81	
olF [g OC kg^{-1}]	Basalt: 0.68 g kg^{-1}	+ 0.45 * SOC
	Loess: 0.68 g kg^{-1}	− 2.58 * Fe_{ox}
	Red Sandstone: 0.68 g kg^{-1}	
	Shell Lime Stone: 0.68 g kg^{-1}	
	Tertiary Sand: 0.68 g kg^{-1}	
	Subsoil (first subsoil horizon)	
SOC [g OC kg^{-1}]	Basalt: 0.93 g kg^{-1}	+ 3.22 * Fe_{ox}
	Loess: 1.04 g kg^{-1}	
	Red Sandstone: 2.28 g kg^{-1}	
	Shell Lime Stone: 7.79 g kg^{-1}	
	Tertiary Sand: 11.03 g kg^{-1}	
C_{mic} [mg kg^{-1}]	Basalt: 64.74 mg kg^{-1}	+ 6.72 * SOC
	Loess: 64.74 mg kg^{-1}	
	Red Sandstone: 64.74 mg kg^{-1}	
	Shell Lime Stone: 64.74 mg kg^{-1}	
	Tertiary Sand: 64.74 mg kg^{-1}	
olF [g OC kg^{-1}]	Basalt: 1.10 g kg^{-1}	+ 0.24 * SOC
	Loess: 0.97 g kg^{-1}	− 0.55 * Fe_{ox}

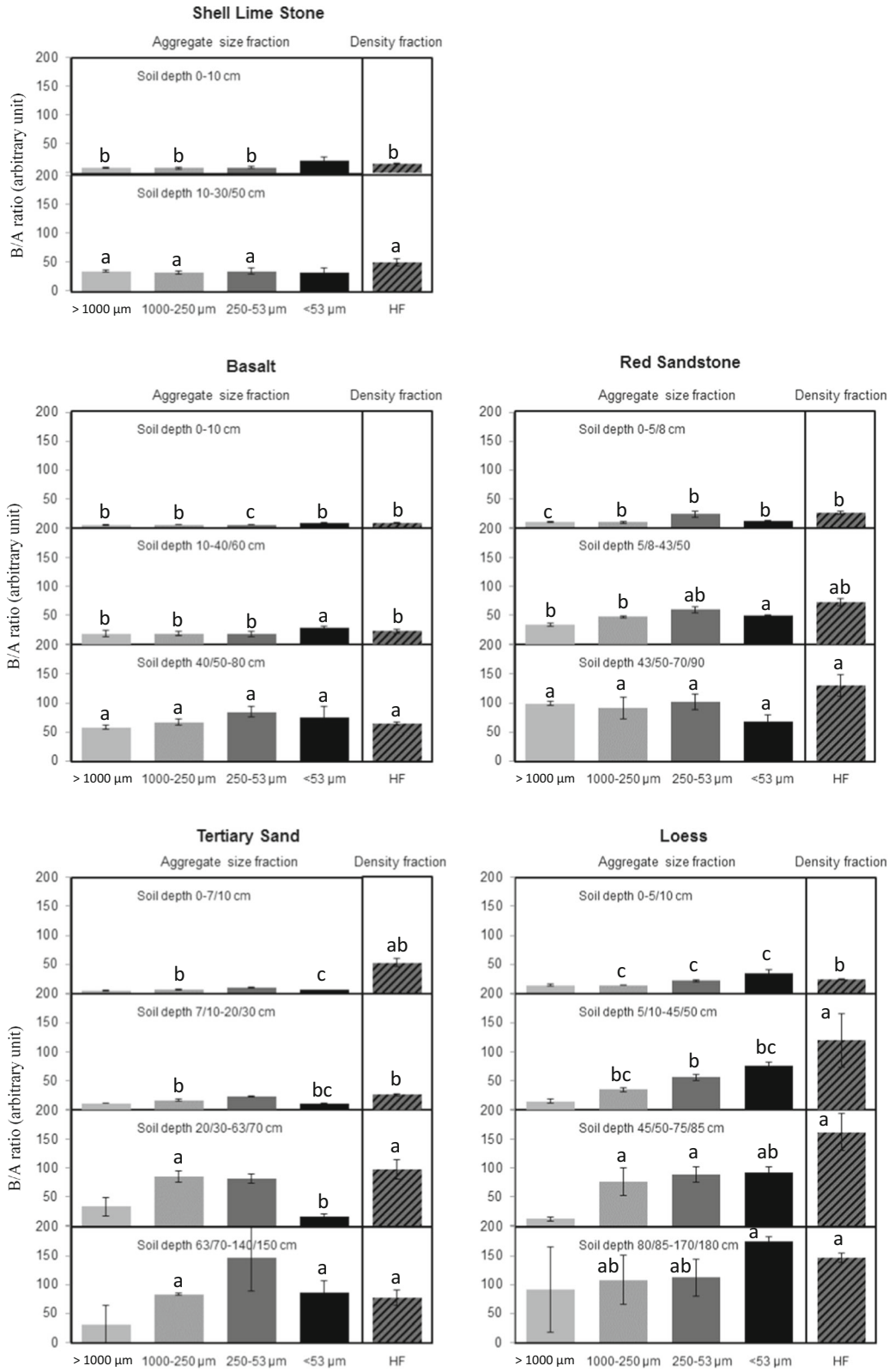
Shell Lime Stone
Aggregate size fraction
Density fraction
B/A ratio (arbitrary unit)
Soil depth 0-10 cm
Soil depth 10-30/50 cm
> 1000 µm
1000-250 µm
250-53 µm
<53 µm
HF
Basalt
Soil depth 0-10 cm
Soil depth 10-40/60 cm
Soil depth 40/50-80 cm
Red Sandstone
Soil depth 0-5/8 cm
Soil depth 5/8-43/50
Soil depth 43/50-70/90
Tertiary Sand
Soil depth 0-7/10 cm
Soil depth 7/10-20/30 cm
Soil depth 20/30-63/70 cm
Soil depth 63/70-140/150 cm
Loess
Soil depth 0-5/10 cm
Soil depth 5/10-45/50 cm
Soil depth 45/50-75/85 cm
Soil depth 80/85-170/180 cm

attributed to interactions between such oxides and reactive organic moieties (Kleber et al. 2015) and the functioning of Fe-oxides as cementing agent within the formation of micro-aggregates (Totsche et al. 2018). Both reaction pathways can lead to accumulation and retention of OC in soil by decreasing its microbial availability. As expected and previously observed (e.g., Rumpel et al. 2002), we also detected for all sites a decrease in the SOC content with soil depth.

Fig. 3 Relative contribution (%) of the organic C (OC) content ▶ separated with aggregate size fractions and the density fractions (g C kg^{-1} soil) from the horizon specific soil samples of the five study sites to the respective bulk soil C (SOC) content. Error bars are standard errors from three field replicates (except Basalt 40/50–80 and Loess 80/85–170/180 with n = 2). Different letters indicate significant differences between depths

Relative proportions of topsoil organic C in aggregate size and density fractions

Macro-aggregates are of major importance for the SOC storage in topsoils under mature beech forest

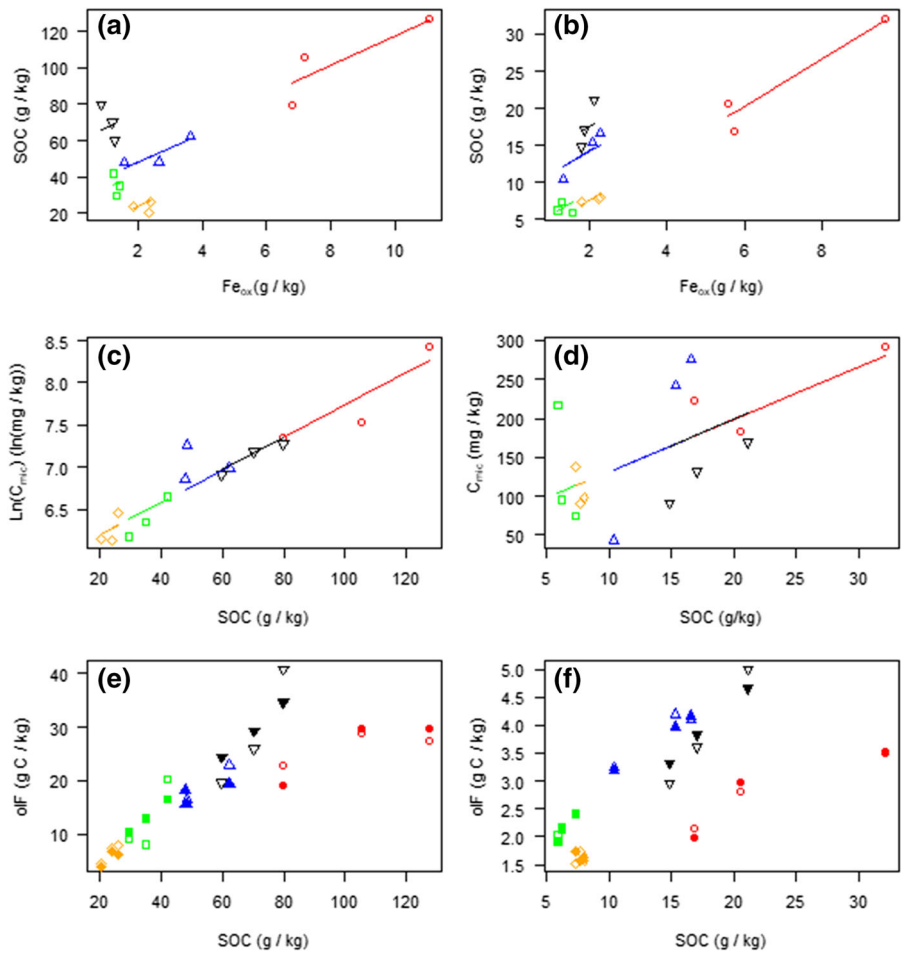

Fig. 2 Measured (open symbols) and modelled (lines in **a** to **d** and closed symbols in **e** and **f**) values using mixed effects models for bulk soil organic C (SOC) against the content of oxalate soluble Fe (Fe_{ox}) in the topsoil (**a**) and subsoil (here and following: first subsoil horizon) (**b**); for log-transformed microbial biomass C (C_{mic}) against SOC in the topsoil (**c**) and for C_{mic} against SOC in the subsoil (**d**); and for the organic C separated with the occluded light fraction (olF) against SOC in the topsoil (**e**) and subsoil (**f**). The open symbols refer to the sites Basalt (red circles), Red Sandstone (green squares), Loess (orange diamonds), Shell Lime Stone (blue triangles pointing up) and Tertiary Sand (black triangles pointing down). (Color figure online)

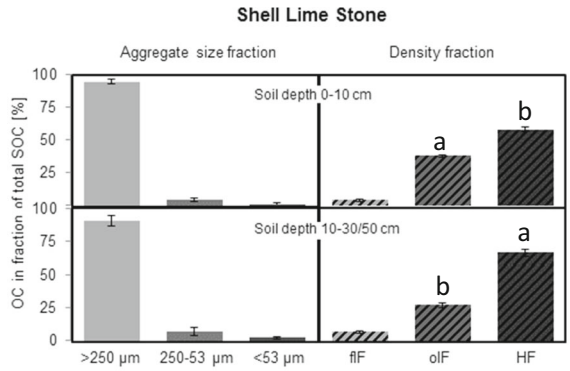
Shell Lime Stone
Aggregate size fraction
Density fraction
OC in fraction of total SOC [%]
Soil depth 0-10 cm
Soil depth 10-30/50 cm
>250 µm
250-53 µm
<53 µm
fIF
oIF
HF

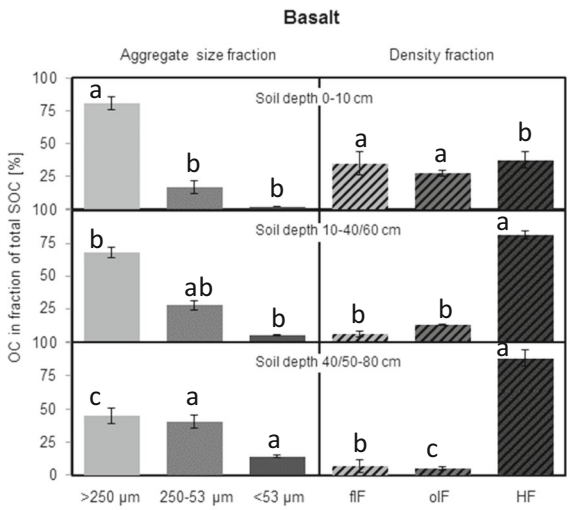
Basalt
Aggregate size fraction
Density fraction
OC in fraction of total SOC [%]
Soil depth 0-10 cm
Soil depth 10-40/60 cm
Soil depth 40/50-80 cm
>250 µm
250-53 µm
<53 µm
fIF
oIF
HF

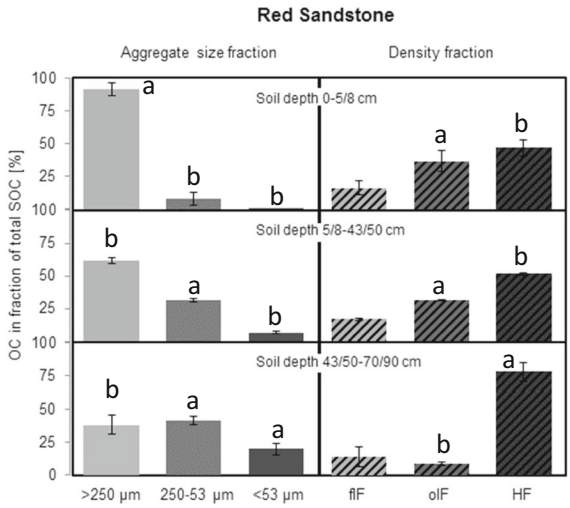
Red Sandstone
Aggregate size fraction
Density fraction
OC in fraction of total SOC [%]
Soil depth 0-5/8 cm
Soil depth 5/8-43/50 cm
Soil depth 43/50-70/90 cm
>250 µm
250-53 µm
<53 µm
fIF
oIF
HF

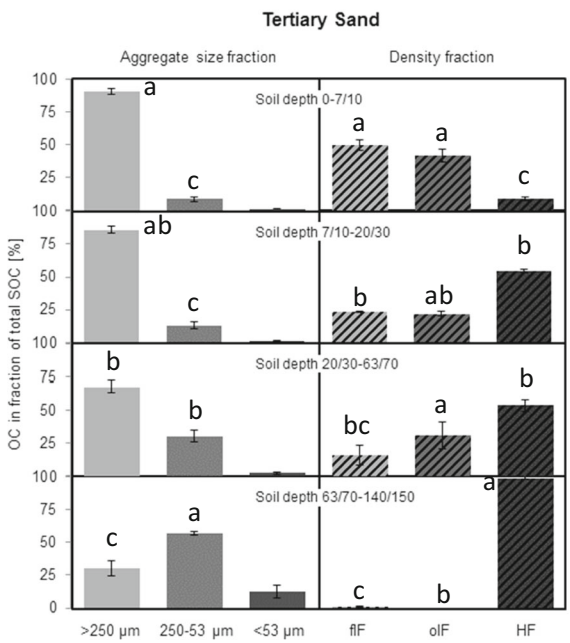
Tertiary Sand
Aggregate size fraction
Density fraction
OC in fraction of total SOC [%]
Soil depth 0-7/10
Soil depth 7/10-20/30
Soil depth 20/30-63/70
Soil depth 63/70-140/150
>250 µm
250-53 µm
<53 µm
fIF
oIF
HF

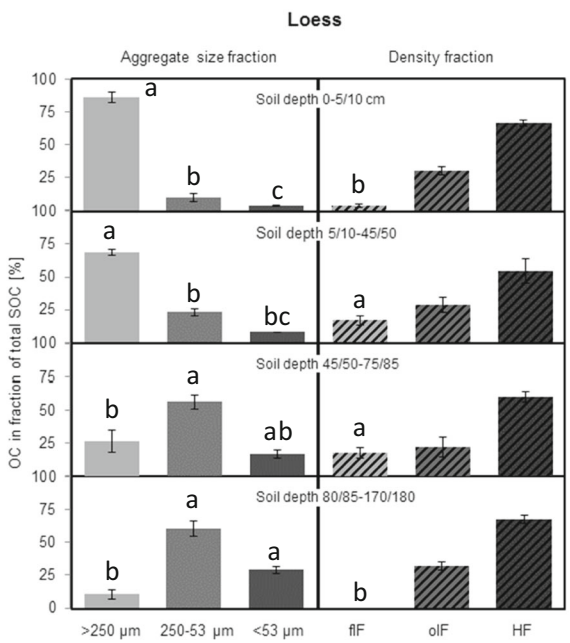
Loess
Aggregate size fraction
Density fraction
OC in fraction of total SOC [%]
Soil depth 0-5/10 cm
Soil depth 5/10-45/50
Soil depth 45/50-75/85
Soil depth 80/85-170/180
>250 µm
250-53 µm
<53 µm
fIF
oIF
HF

independent of the soil type and parent material. In the analysed topsoil horizons covering a depth range from 0 to 10 cm, 81 to 94% of the SOC was stored within both macro-aggregate fractions (> 1000 µm fraction + 1000–250 µm fraction). We observed 4 to 17% of the SOC to be stored in micro-aggregates (250–53 µm) and 0.6 to 4% of the SOC in the silt and clay sized fraction (< 53 µm) (Fig. 3). Based on the inverse relationship between aggregate size and the stability of the associated OM (Tisdall and Oades 1982; John et al. 2005; Liao et al. 2006), only the small proportion of the OC that is associated with aggregates < 53 µm can be considered as effectively stabilized against microbial decomposition by aggregation processes and mineral association in the forest topsoils under study. These results suggest that a majority of topsoil SOC under mature beach forest is prone to short-term decomposition losses in case of disturbance, such as land use change.

Compared to the data of aggregate size fractionation, the results from density fractionation pointed towards higher proportions of SOC protected from microbial decomposition in the studied forest topsoils. The flF, which mainly represents non-aggregated and easily microbial available plant particles, accounted for 4 to 50% of the SOC leaving a major part in the olF and HF density fractions, which are indicative for OM stronger protected against microbial decomposition (John et al. 2005; Marin-Spiotta et al. 2008). The olF (27–42% of SOC) represents aggregate occluded plant particles (Wagai et al. 2009) and the HF (9–66% of SOC) accounts for OM that is associated with the soil mineral phase (Sollins et al. 2009; Hatton et al. 2012; Pronk et al. 2012). Based on extraction principles, the olF recovers organic particles released from aggregates of different size being disrupted during density fractionation and the HF recovers mineral associated OM that is not aggregate occluded and, similar to the olF, part of aggregates of different size. Consequently, the proportion of SOC protected against microbial decomposition by aggregate occlusion and mineral association in mineral topsoil under mature beech forest might be underestimated if only the fraction < 53 µm is taken into account. Our data also imply that the proportions of SOC stronger protected against microbial decay were higher in soils derived from Loess and Lime Stone than in soils derived from Tertiary Sand and Basalt (Fig. 3).

Relative proportions of subsoil organic C in aggregate size and density fractions

Our data indicated a site independent increase in the proportion of OC stabilized by aggregation processes at the micro-scale, especially for non-sandy soils (i.e. excluding Tertiary Sand soil) with depths larger than 50 cm (i.e. excluding Lime Stone soil) for which the majority of significant differences was detected. Macro-aggregates (> 250 µm) accounted for the majority of the SOC (61–91%) in the first subsoil horizon (5–60 cm), which is in agreement with data from Xiang et al. (2015) and Schwendemann and Pendall (2006) for forest soils developed from Sandstone, Shell, and Andesit. However, for four out of five soils, we detected a significant decrease in the relative SOC proportion of macro-aggregate associated OC and an increase of micro-aggregate (< 250 µm) associated OC with soil depth (Fig. 3).

The effect of soil depth on SOC proportions of density fractions seems to be more site specific as compared with the aggregate size fractions. For the Basalt and Tertiary Sand soil, the relative SOC proportions of flF significantly decreased with increasing soil depth (Fig. 3) confirming results from Angst et al. (2016). For the Loess soil, however, we found a significant increase from 4% in the topsoil to 17–18% in the first and second subsoil horizon (depth range 5–85 cm). This increase might be derived from higher bioturbation and better conditions for root growth in the Loess subsoil compared to the other subsoils under study. This is corroborated by the lower relative decline in root biomass for the Loess soil compared to the Basalt and Tertiary Sand soil as determined by Angst et al. (2018).

The relative SOC proportions of the olF significantly decreased with soil depth for all but the Loess soil (Fig. 3) confirming for the latter the larger and highly site specific importance of plant derived organic particles (i.e. flF and olF) for the SOC storage across the soil profile. In general, aggregate occluded organic particles as separated with the olF accounted for 8 to 31% of the SOC in the first two subsoil horizons (5–90 cm) of the study sites. Slightly lower values (4–17%) were found by Schrumpf et al. (2013) for subsoil samples (10–60 cm) from three different soils under broadleaf forest, which might be derived from the lower density cut off the authors used for the olF separation (1.6 g cm^{-3} vs. 1.8 g cm^{-3}).

We found a generally site independent increase in the proportion of SOC that is present in mineral associated form under mature beech forest down the profile because for four out of five soils (i.e., except the Loess soil) a significant increase in HF-SOC proportions with soil depth was detected (Fig. 3). Similar to the topsoils, a considerable higher proportion of OC might be considered as stabilized if the HF (52–88% in the first two subsoil horizons (5–90 cm) and 68–99% in the third subsoil horizon (60–180 cm)) is considered rather than the < 53 µm fraction.

Stabilization and destabilization of organic matter with increasing soil depths: reconciling fractionation data with FTIR, CO_2 and microbial biomass C measurements

Our data suggest that the increase of the relative proportion of stabilized OM as well as the decrease of the relative proportion of easily available OM with soil depth seem to be largely independent of soil type or parent material under mature beech forest. Based on the current understanding, OM associated with macro-aggregates (> 250 µm) and with the flF can be considered to be less protected against microbial decomposition leading to its importance as substrate and nutrient source for fungi and bacteria. In contrast, OM associated with aggregates < 53 µm and with the HF was shown to be stronger protected against microbial decomposition by occlusion in mechanically more stable aggregates and interactions with soil mineral surfaces causing its larger relevance for long-term SOC storage. For the analysed five soil profiles, we observed in general a decrease in the relative SOC proportions of macro-aggregates or the flF with soil depth (Fig. 3). In contrast, we detected a general increase in the relative SOC proportions of the < 53 µm fraction or the HF with increasing soil depth (Fig. 3).

Data from incubation experiments and from microbial biomass measurements suggest an increase in the relative proportion of labile OM with soil depth raising questions about the long-term stabilization of OM against microbial decomposition in the subsoil. As expected, we observed a decrease in the cumulative CO_2-C emissions after 14 days and in the C_{mic} contents with increasing soil depth. However, the CO_2-C/SOC and CO_2-C/C_{mic} ratios are generally increasing with soil depth, which is in line with results from other studies (Joergensen et al. 2002; Agnelli et al. 2004; Salomé et al. 2010; Wordell-Dietrich et al. 2016). This resulted in distinctly lower CO_2-C/SOC and CO_2-C/C_{mic} ratios especially in the topsoil horizons (depth range 0–10 cm) of the Loess and the Tertiary Sand soil as compared with those of the respective deepest subsoil horizons (depth range 70–180 cm).

The detected simultaneous trends of a relative increase in more stabilized OM and a relative increase in easily decomposable OM is exemplified by the third subsoil horizon of the Tertiary Sand soil with 99% of the SOC associated with the HF and about 2% of the SOC to be respired within 14 days. In contrast, the respective topsoil showed about 9% of the SOC to be associated with the HF and 0.4% to be respired in the same time. An explanation might be that the < 53 µm fraction and the HF fueling the easily available OM in the subsoil, which is corroborated by data from Tan et al. (2013) and Fang et al. (2015). There is increasing evidence that mineral-associated OM is not stable per se but contains a certain proportion of fast cycling, microbial accessible OC (e.g., Mikutta and Kaiser 2011; Torn et al. 2013; Gabriel et al. 2018). In absence of otherwise more easily available OM in form of flF, for example, OM associated with HF or the < 53 µm fraction might become even more relevant as substrate for microorganisms in the nutrient scarce subsoil. However, differences in the micro-biome between topsoil and subsoil and microbial adaption mechanisms to the oligotrophic subsoil environment that might also affect OM decomposition patterns are still largely unknown (Brewer et al. 2019).

Further support for microbially processed OM associated with stabilized fractions down the profile is provided by the FTIR data. In general, the B/A ratios of the OM associated with the aggregate size fractions and the HF are increasing with an increase in soil depth (Fig. 1). The magnitude of the B/A ratio as a measure for the relative C=O group content of the OM tends to vary as a function of the degree of microbial oxidative decomposition (adding oxygen containing functional groups to the processed substrate) and as a function of the concentration of amides (containing carbonyl groups) as derived from proteinaceous microbial debris (e.g., Kaiser et al. 2014). Therefore, the increase in the B/A ratio with soil depth suggests an increasing proportion of microbially derived and increasingly

microbially processed OM across different OM fractions.

Conclusions

Analyzing genetic topsoil and subsoil horizons of five different soils under mature broadleaf forest revealed with increasing depth a significant increase in the proportions of the SOC that is occluded within microaggregates < 53 µm for three soils (except Tertiary Sand and Lime Stone soil) or associated with the mineral phase (HF) for four soils (except Loess). In conclusion, the soil depth specific relative importance of OM stabilization mechanisms seems to be influenced by the soil parent material, which needs to be considered in the assessment of the soil C sequestration potential of a specific forest type covering an area with heterogenic soil forming substrate. If implemented, such parent material specific data will improve the accuracy of predictions made within terrestrial C models. Parallel to larger relative proportions of OC in fractions assumed to recover stabilized OM with increasing soil depth we found indications for an increase in relative proportions of labile OM. Here, OM associated with the < 53 µm fraction and HF seems to become more important as a substrate for microorganisms with increasing soil depth, which might reduce the mean residence time of OC in the subsoil.

Acknowledgements The study was funded by the Deutsche Forschungsgemeinschaft (Research Group 1806 'The Forgotten Part of Carbon Cycling: Organic Matter Storage and Turnover in Subsoils (SUBSOM)'). We thank Anja Sawallisch and Gabriele Dormann, University of Kassel, for technical assistance and we are very grateful to Dr. Peter Schad, Technical University München, for his support with the classification of soil types and soil horizons.

References

Agnelli A, Ascher J, Corti G, Ceccherini MT, Nannipieri P, Pietramellara G (2004) Distribution of microbial communities in a forest soil profile investigated by microbial biomass, soil respiration and DGGE of total and extracellular DNA. Soil Biol Biochem 36:859–868. https://doi.org/10.1016/j.soilbio.2004.02.004

Angst G, Kögel-Knabner I, Kirfel K, Hertel D, Mueller CW (2016) Spatial distribution and chemical composition of soil organic matter fractions in rhizosphere and non-rhizosphere soil under European beech (*Fagus sylvatica* L.). Geoderma 264:179–187. https://doi.org/10.1016/j.geoderma.2015.10.016

Angst G, Messinger J, Greiner M, Häusler W, Hertel D, Kirfel K, Kögel-Knabner I, Leuschner C, Rethemeyer J, Mueller CW (2018) Soil organic carbon stocks in topsoil and subsoil controlled by parent material, carbon input in the rhizosphere, and microbial-derived compounds. Soil Biol Biochem 122:19–30

Baldock JA, Skjemstad JO (2000) Role of the soil matrix and minerals in protecting natural organic materials against biological attack. Org Geochem 31:697–710. https://doi.org/10.1016/S0146-6380(00)00049-8

Batjes NH (1996) Total carbon and nitrogen in the soils of the world. Eur J Soil Sci 47:151–163. https://doi.org/10.1111/j.1365-2389.1996.tb01386.x

Brewer TE, Aronson EL, Arogyaswamy K, Billings SA, Botthoff JK, Campbell AN, Dove NC, Fairbanks D, Gallery RE, Hart SC, Kaye J, King G, Logan G, Lohse KA, Maltz MR, Mayorga E, O'Neill C, Owens SM, Packman A, Pett-Ridge J, Plante AF, Richter DD, Silver WL, Yang WH, Fierer N (2019) Ecological and genomic attributes of novel bacterial taxa that thrive in subsurface soil horizons. mBio 10:e01318–e1319. https://doi.org/10.1128/mBio.01318-19

Brookes PC, Landman A, Pruden G, Jenkinson DS (1985) Chloroform fumigation and the release of soil nitrogen: a rapid direct extraction method to measure microbial biomass nitrogen in soil. Soil Biol Biochem 17:837–842. https://doi.org/10.1016/0038-0717(85)90144-0

Cambardella CA, Elliott ET (1993) Carbon and nitrogen distribution in aggregates from cultivated and native grassland soils. Soil Sci Soc Am J 57:1071–1076. https://doi.org/10.2136/sssaj1993.03615995005700040032x

Cerli C, Celi L, Kalbitz K, Guggenberger G, Kaiser K (2012) Separation of light and heavy organic matter fractions in soil—testing for proper density cut-off and dispersion level. Geoderma 170:403–416. https://doi.org/10.1016/j.geoderma.2011.10.009

DIN 19684-6 (1997) Bodenuntersuchungsverfahren im Landwirtschaftlichen Wasserbau - Chemische Laboruntersuchungen - Teil 6: Bestimmung des Gehaltes an oxalatlöslichem Eisen. DIN 19684-6, Beuth Verlag, Berlin, p. 1997-12

DIN ISO 11277 (2002) Bodenbeschaffenheit - Bestimmung der Partikelgrößenverteilung in Mineralböden - Verfahren mittels Siebung und Sedimentation. ISO 11277: 1998/Cor.1:2002, Beuth Verlag Berlin

Don A, Schumacher J, Freibauer A (2011) Impact of tropical land-use change on soil organic C stocks—a meta-analysis. Glob Chang Biol 17:1658–1670. https://doi.org/10.1111/j.1365-2486.2010.02336.x

Ellerbrock RH, Gerke HH (2013) Characterization of organic matter composition of soil and flow path surfaces based on physiochemical principles—a review. Adv Agron 121:117–177. https://doi.org/10.1016/B978-0-12-407685-3.00003-7

Eusterhues K, Rumpel C, Kögel-Knabner I (2005) Organo-mineral associations in sandy acid forest soils: importance of specific surface area, iron oxides and micropores. Eur J Soil Sci 56:753–763. https://doi.org/10.1016/j.orggeochem.2005.06.010

Fang X-M, Chen F-S, Wan S-Z, Yang Q-P, Shi J-M (2015) Topsoil and deep soil organic carbon concentration and stability vary with aggregate size and vegetation type in subtropical China. PLoS ONE 10(9):e0139380. https://doi.org/10.1371/journal.pone.0139380

Feng W, Shi Z, Jiang J, Xia J, Liang J, Zhou J, Luo Y (2016) Methodological uncertainty in estimating carbon turnover times of soil fractions. Soil Biol Biochem 100:118–124. https://doi.org/10.1016/j.soilbio.2016.06.003

Gabriel CE, Kellman L, Prest D (2018) Examining mineral-associated soil organic matter pools through depth in harvested forest soil profiles. PLoS ONE 13:e0206847. https://doi.org/10.1371/journal.pone.0206847

Golchin A, Oades JM, Skjemstad JO, Clarke P (1994) Study of free and occluded particulate organic matter in soils by solid state ^{13}C CP-MAS NMR spectroscopy and scanning electron microscopy. Aust J Soil Res 32:285–309. https://doi.org/10.1071/SR9940285

Hatton P-J, Kleber M, Zeller B, Moni C, Plante AF, Townsend K, Gelhaye L, Derrien KLD (2012) Transfer of litter-derived N to soil mineral-organic associations: evidence from decadal ^{15}N tracer experiments. Org Geochem 42:1489–1501. https://doi.org/10.1016/j.orggeochem.2011.05.002

Heinze S, Oltmanns M, Joergensen RG, Raupp J (2011) Changes in microbial biomass indices after 10 years of farmyard manure and vegetal fertilizer application to a sandy soil under organic management. Plant Soil 343:221–234. https://doi.org/10.1007/s11104-010-0712-8

Hijmans RJ, Cameron SE, Parra JL, Jones PG, Jarvis A (2005) Very high resolution interpolated climate surfaces for global land areas. Intern J Clim 25:1965–1978. https://doi.org/10.1002/joc.1276

Isermeyer H (1952) Eine einfache Methode zur Bestimmung der Bodenatmung und der Karbonate im Boden. Z Pflanzenernähr Bodenkd 56:26–38. https://doi.org/10.1002/jpln.19520560107

IUSS Working Group WRB (2006) World reference base for soil resources 2006. World Soil Resources Reports No. 103. FAO, Rome

Jacobs A, Helfrich M, Hanisch S, Quendt U, Rauber R, Ludwig B (2010) Effect of conventional and minimum tillage on physical and biochemical stabilization of soil organic matter. Biol Fertil Soils 46:671–680. https://doi.org/10.1007/s00374-010-0472-x

Jacobs A, Rauber R, Ludwig B (2009) Impact of reduced tillage on carbon and nitrogen storage of two Haplic Luvisols after 40 years. Soil Tillage Res 102:158–164. https://doi.org/10.1016/j.still.2008.08.012

Jain AK, Yang X (2005) Modeling the effects of two different land cover change data sets on the carbon stocks of plants and soils in concert with CO_2 and climate change. Glob Biogeochem Cycles 19:1–20. https://doi.org/10.1029/2004GB002349

Joergensen RG, Raubuch M, Brandt M (2002) Soil microbial properties down the profile of a black earth burie by colluvium. J Plant Nutr Soil Sci 165:274–280

John B, Yamashita T, Ludwig B, Flessa H (2005) Storage of organic carbon in aggregate and density fractions of silty soils under different types of land use. Geoderma 128:63–79. https://doi.org/10.1016/j.geoderma.2004.12.013

Kaiser K, Eusterhues K, Rumpel C, Guggenberger G, Kögel-Knabner I (2002) Stabilization of organic matter by soil minerals – investigations of density and particle-size fractions from two acid forest soils. J Plant Nutr Soil Sci 165:451–459

Kaiser M, Walter K, Ellerbrock RH, Sommer M (2011) Effects of land use and mineral characteristics on the organic carbon content, and the amount and composition of Na-pyrophosphate-soluble organic matter, in subsurface soils. Eur J Soil Sci 62:226–236. https://doi.org/10.1111/j.1365-2389.2010.01340.x

Kaiser M, Ellerbrock RH, Wulf M, Dultz S, Hierath C, Sommer M (2012) The influence of mineral characteristics on organic matter content, composition, and stability of topsoils under long-term arable and forest land use. J Geophys Res 117:G02018. https://doi.org/10.1029/2011JG001712

Kaiser M, Ghezzehei TA, Kleber M, Myrold DD, Berhe AA (2014) Influence of calcium carbonate and charcoal applications on organic matter storage in silt-sized aggregates formed during a microcosm experiment. Soil Sci Soc Am J 78:1624–1631. https://doi.org/10.2136/sssaj2014.04.0146

Kleber M, Eusterhues K, Keiluweit M, Mikutta C, Mikutta R, Nico PS (2015) Mineral-organic associations: formation, properties, and relevance in soil environments. Adv Agron 130:1–140. https://doi.org/10.1016/bs.agron.2014.10.005

Kramer MG, Sandermann J, Chadwick OA, Chorover J, Vitousek PM (2012) Long-term carbon storage through retention of dissolved aromatic acids by reactive particles in soil. Glob Chang Biol 18:2594–2605. https://doi.org/10.1111/j.1365-2486.2012.02681.x

Liao JD, Boutton TW, Jastrow JD (2006) Organic matter turnover in soil physical fractions following woody plant invasion of grassland: evidence from natural ^{13}C and ^{15}N. Soil Biol Biochem 38:3197–3210. https://doi.org/10.1016/j.soilbio.2006.04.004

Loeppert RH and Suarez DL (1996) Carbonate and gypsum. In: Sparks DL et al (eds) Methods of soil analysis. Part 3. Chemical methods. ASA and SSSA, Madison, pp 437–474

Marín-Spiotta E, Swanston CW, Torn MS, Silver WL, Burton SD (2008) Chemical and mineral control of soil carbon turnover in abandoned tropical pastures. Geoderma 143:49–62. https://doi.org/10.1016/j.geoderma.2007.10.001

McFarlane KJ, Torn MS, Hanson PJ, Porras RC, Swantson CW, Callaham MA Jr, Guilderson TP (2013) Comparison of soil organic matter dynamics at five temperate deciduous forests with physical fractionation and radiocarbon measurements. Biogeochemistry 112:457–476. https://doi.org/10.1007/s10533-012-9740-1

Mehra OP and Jackson ML (1960) Iron oxide removal from soils and clays by a dithionite-citrate system buffered with sodium bicarbonate. Clays and Clay Minerals, 7th national conference on clays and clay minerals, Washington, D.C. vol 7, pp 317–327. https://doi.org/10.1346/CCMN.1958.0070122

Mikutta R, Kaiser K (2011) Organic matter bound to mineral surfaces: resistance to chemical and biological oxidation.

Soil Biol Biochem 43:1738–1741. https://doi.org/10.1016/j.soilbio.2011.04.012

Mikutta R, Kleber M, Torn MS, Jahn R (2006) Stabilization of soil organic matter: association with minerals or chemical recalcitrance? Biogeochemistry 77:25–56. https://doi.org/10.1007/s10533-005-0712-6

Mobley ML, Lajtha K, Kramer MG, Bacon AR, Heine PR, Richter DD (2015) Surficial gains and subsoil losses of soil carbon and nitrogen during secondary forest development. Glob Change Biol 21:986–996. https://doi.org/10.1111/gcb.12715

North PF (1976) Towards an absolute measurement of soil structural stability using ultrasound. Eur J Soil Sci 27:451–459. https://doi.org/10.1111/j.1365-2389.1976.tb02014.x

Paul EA, Collins HP, Leavitt SW (2001) Dynamics of resistant soil carbon of midwestern agricultural soils measured by naturally occurring C-14 abundance. Geoderma 104:239–256. https://doi.org/10.1016/S0016-7061(01)00083-0

Piepho HP, Büchse A, Richter C (2004) A mixed modelling approach to randomized experiments with repeated measures. J Agron Crop Sci 190:230–247. https://doi.org/10.1111/j.1439-037X.2004.00097.x

Post WM, Emanuel WR, Zinke PJ, Stangenberger AG (1982) Soil carbon pools and world life zones. Nature 298:156–159. https://doi.org/10.1038/298156a0

Post WM, Kwon KC (2000) Soil C sequestration and land-use change: processes and potential. Glob Change Biol 6:317–327. https://doi.org/10.1046/j.1365-2486.2000.00308.x

Powers JS, Corre MD, Twine TE, Veldkamp E (2011) Geographic bias of field observations of soil carbon stocks with tropical land-use changes precludes spatial extrapolation. PNAS 108:6318–6322. https://doi.org/10.1073/pnas.1016774108

Pronk GJ, Heister K, Ding G-C, Smalla K, Kögel-Knabner I (2012) Development of biogeochemical interfaces in an artificial soil incubation experiment; aggregation and formation of organo-mineral associations. Geoderma 189–190:585–594. https://doi.org/10.1016/j.geoderma.2012.05.020

R Core Team (2017) R: a language and environment for statistical computing. R Foundation for Statistical Computing, Vienna

Rasse DP, Mulder J, Moni C, Chenu C (2006) Carbon turnover kinetics with depth in a French loamy soil. Soil Sci Soc Am J 70:2097–2105. https://doi.org/10.2136/sssaj2006.0056

Ren F, Sun N, Xu M, Zhang X, Wu L, Xu M (2019) Changes in soil microbial biomass with manure application in cropping systems: a meta-analysis. Soil Till Res 194:104291. https://doi.org/10.1016/j.still.2019.06.008

Rumpel C, Kögel-Knabner I (2011) Deep soil organic matter—a key but poorly understood component of terrestrial C cycle. Plant Soil 338:143–158. https://doi.org/10.1007/s11104-010-0391-5

Rumpel C, Kögel-Knabner I, Bruhn F (2002) Vertical distribution, age, and chemical composition of organic carbon in two forest soils of different pedogenesis. Org Geochem 33:1131–1142. https://doi.org/10.1016/S0146-6380(02)00088-8

Salomé C, Nunan N, Pouteau V, Lerch TZ, Chenu C (2010) Carbon dynamics in topsoil and in subsoil may be controlled by different regulatory mechanisms. Glob Chang Biol 16:416–426. https://doi.org/10.1111/j.1365-2486.2009.01884.x

Sánchez-de Léon Y, Lugo-Pérez J, Wise DH, Jastrow JD, Gónzales-Meler MA (2014) Aggregate formation and carbon sequestration by earthworms in soil from temperate forest exposed to elevated atmospheric CO_2: a microcosm experiment. Soil Biol Biochem 68:223–230. https://doi.org/10.1016/jsoilbio.2013.09.023

SAS Institute Inc (2014) SAS/STAT®13.2 User's guide: high-performance procedures. SAS Institute Inc., Cary

Schmidt MWI, Torn MS, Abiven S, Dittmar T, Guggenberger G, Janssens IA, Kleber M, Kögel-Knabner I, Lehmann J, Manning DAC, Nannipieri P, Rasse DP, Weiner S, Trumbore SE (2011) Persistence of soil organic matter as an ecosystem property. Nature 478:49–56. https://doi.org/10.1038/nature10386

Schrumpf M, Kaiser K (2015) Large differences in estimates of soil organic carbon turnover in density fractions by using single and repeated radiocarbon inventories. Geoderma 239:168–178. https://doi.org/10.1016/j.geoderma.2014.09.025

Schrumpf M, Kaiser K, Guggenberger G, Persson T, Kögel-Knabner I, Schulze E-D (2013) Storage and stability of organic carbon in soils as related to depth, occlusion within aggregates, and attachment to minerals. Biogeosciences 10:1675–1691. https://doi.org/10.5194/bg-10-1675-2013

Schwendemann L, Pendall E (2006) Effects of forest conversion into grassland on soil aggregate structure and carbon storage in Panama: evidence from soil carbon fractionation and stable isotopes. Plant Soil 288:217–232. https://doi.org/10.1007/s11104-006-9109-0

Sollins P, Kramer MG, Swantson C, Lajtha K, Filley T, Aufdenkampe AK, Wagai R, Bowden RD (2009) Sequential density fractionation across soils of contrasting mineralogy: evidence for both microbial- and mineral-controlled soil organic matter stabilization. Biogeochemistry 96:209–231. https://doi.org/10.1007/s10533-009-9359-z

Tan W, Zhou L, Liu K (2013) Soil aggregate fraction-based ^{14}C analysis and its application in the study of soil organic carbon turnover under forests of different ages. Chin Sci Bull 58:1936–1947. https://doi.org/10.1007/s11434-012-5660-7

Tisdal JM, Oades JM (1982) Organic matter and water-stable aggregates in soils. J Soil Sci 33:141–163. https://doi.org/10.1111/j.1365-2389.1982.tb01755.x

Totsche KU, Amelung W, Gerzabek MH, Guggenberger G, Klumpp E, Knief C, Lehndorff E, Mikutta R, Peth S, Prechtel A, Ray N, Kögel-Knabner I (2018) Microaggregates in soils. J Plant Nutr Soil Sci 181:104–136. https://doi.org/10.1002/jpln.201600451

Torn MS, Kleber M, Zavaleta ES, Zhu B, Field CB, Trumbore SE (2013) A dual isotope approach to isolate soil carbon pools of different turnover times. Biogeosciences 10:8067–8081. https://doi.org/10.5194/bg-10-8067-2013

Torres-Sallan G, Creamer RE, Lanigan GJ, Reidy B, Byrne KA (2018) Effects of soil type and depth on carbon distribution within soil macroaggregates from temperate grassland

systems. Geoderma 313:52–56. https://doi.org/10.1016/j.geoderma.2017.10.012

Vancampenhout K, De Vos B, Wouters K, Swennen R, Buurman P, Deckers J (2012) Organic matter of subsoil horizons under broadleaved forest: highly processed or labile and plant-derived? Soil Biol Biochem 50:40–46. https://doi.org/10.1016/j.soilbio.2012.03.005

Vance ED, Brookes PC, Jenkinson DS (1987) An extraction method for measuring soil microbial biomass C. Soil Biol Biochem 19:703–707. https://doi.org/10.1016/0038-0717(87)90052-6

Wade AM, Richter DD, Mdjibe VP, Bacon AR, Heine PR, White LJT, Poulsen JR (2019) Estimates and determinants of stocks of deep soil carbon in Gabon, Central Africa. Geoderma 341:236–248. https://doi.org/10.1016/j.geoderma.2019.01.004

Wagai R, Mayer LM, Kitayama K (2009) Nature of the "occluded" low-density fraction in soil organic matter studies: a critical review. Soil Sci Plant Nutr 55:13–25. https://doi.org/10.1111/j.1747-0765.2008.00356.x

West TO, Post WM (2002) Soil organic carbon sequestration rates by tillage and crop rotation: a global data analysis. Soil Sci Soc Am J 66:1930–1946. https://doi.org/10.2136/sssaj2002.1930

Wiseman CLS, Püttmann W (2006) Interactions between mineral phases in the preservation of soil organic matter. Geoderma 134:109–118. https://doi.org/10.1016/j.geoderma.2005.09.001

Wordell-Dietrich P, Don A, Helfrich M (2016) Controlling factors for the stability of subsoil carbon in a Dystric Cambisol. Geoderma. https://doi.org/10.1016/j.geoderma.2016.08.023

Wu J, Joergensen RG, Pommerening B, Chaussod R, Brookes PC (1990) Measurement of soil microbial biomass C by fumigation-extraction—an automated procedure. Soil Biol Biochem 22:1167–1169. https://doi.org/10.1016/0038-0717(90)90046-3

Xiang H, Zhang L, Wen D (2015) Change of soil carbon fractions and water-stable aggregates in a forest ecosystem succession in South China. Forests 6:2703–2718. https://doi.org/10.3390/f6082703

Zhao Q, Poulson SR, Obrist D, Sumaila S, Dynes JJ, McBeth JM, Yang Y (2016) Iron-bound organic carbon in forest soils: quantification and characterization. Biogeosciences 13:4777–4788. https://doi.org/10.5194/bg-13-4777-2016